

Investigating Feature Attribution for 5G Network Intrusion Detection

Federica Uccello^a, Simin Nadjm-Tehrani^a

^a*Department of Computer and Information Science, Linköping
University, Linköping, Sweden*

Abstract

With the rise of fifth-generation (5G) networks in critical applications, it is urgent to move from detection of malicious activity to systems capable of providing a reliable verdict suitable for mitigation. In this regard, understanding and interpreting machine learning (ML) models' security alerts is crucial for enabling actionable incident response orchestration. Explainable Artificial Intelligence (XAI) techniques are expected to enhance trust by providing insights into why alerts are raised. A dominant approach statistically associates feature sets that can be correlated to a given alert. This paper starts by questioning whether such attribution is relevant for future generation communication systems, and investigates its merits in comparison with an approach based on logical explanations. We extensively study two methods, SHAP and VoTE-XAI, by analyzing their interpretations of alerts generated by an XGBoost model in three different use cases with several 5G communication attacks. We identify three metrics for assessing explanations: sparsity, how concise they are; stability, how consistent they are across samples from the same attack type; and efficiency, how fast an explanation is generated. As an example, in a 5G network with 92 features, 6 were deemed important by VoTE-XAI for a Denial of Service (DoS) variant, ICMPFlood, while SHAP identified over 20. More importantly, we found a significant divergence between features selected by SHAP and VoTE-XAI. However, none of the top-ranked features selected by SHAP were missed by VoTE-XAI. When it comes to efficiency of providing interpretations, we found that VoTE-XAI is significantly more responsive, e.g. it provides a single explanation in under 0.002 seconds, in a high-dimensional setting (478 features).

Keywords: Security Monitoring, Intrusion Detection, 5G Networks,

1. Introduction

As fifth-generation (5G) networks are deployed in more critical applications, the demand for advanced security mechanisms capable of operating in highly dynamic environments has become more urgent. These mechanisms must be able to detect threats rapidly and respond effectively to evolving attack vectors [1].

Machine Learning (ML) is emerging as a candidate to address complex problems across diverse domains, including healthcare, telecommunications, and autonomous driving [2]. In recent years, the literature has increasingly explored the potential of applying ML techniques in 5G networks, but has also highlighted some limitations [3, 4, 5]. Although the integration of ML into security applications (such as threat intelligence and malware analysis) has shown some potential, in the area of intrusion detection, some challenges still need to be resolved [6, 2].

As in other domains, applying ML to security in 5G settings introduces a range of technical and practical challenges, and a gap remains between theoretical research and practical deployment [7]. The opaque, “black-box” nature of many ML models presents a significant obstacle in environments defined as high-risk under the European Union’s Artificial Intelligence (AI) Act¹, including financial services, healthcare systems, and government infrastructures, many of which may be connected through wireless mobile interfaces.

Regulatory and standardization bodies such as ENISA and NIST emphasize the need for transparency, accountability, and operational readiness in AI-driven security systems [8, 9]. Yet, these principles are rarely addressed along with performance and explainability trade-offs. Explainable Artificial Intelligence (XAI) is essential for exploiting the potential of ML model decision-making and to promote trust by human experts [10, 11]. Interpretability, the ability to explain or justify model predictions in a human-

Email addresses: federica.uccello@liu.se (Federica Uccello),
simin.nadjm-tehrani@liu.se (Simin Nadjm-Tehrani)

¹<https://digital-strategy.ec.europa.eu/en/policies/regulatory-framework-ai>

understandable way [12], is increasingly recognized as crucial in such contexts.

In this regard, tree ensembles offer a practical alternative to complex, black-box models due to their simplicity and clarity in structuring decision paths for classification and regression [13]. According to Chander et al. [14], decision trees can be employed when the features present in a dataset are dependent in nature, as in tabular data, which is the input type to network intrusion detection systems. Moreover, tree ensembles have demonstrated superior predictive performance over neural networks in several real-world, tabular-data applications [15].

In 5G networks, integrating XAI into monitoring systems can help ensure both high accuracy in threat detection and clarity in response generation [16]. Further research is essential to embed models in orchestrators that maintain interpretability without compromising performance aiming at regulation-compliant AI in 5G environments [17].

Note that the current paper does not aim to advance the state of intrusion detection in 5G networks, but assumes that further research can overcome some of the pitfalls of AI-based techniques for identifying attacks and anomalies [7].

Aiming to address further challenges, this study will provide a deeper understanding of the merits and limitations of explainability in the context of security monitoring within 5G networks.

Several techniques are being explored for explainability, including Local Interpretable Model-Agnostic Explanations (LIME) [18], Anchors [19], Counterfactual [20], Integrated Gradient [21], and MaxSAT [22]. Multiple surveys cover the applicability of these methods in various domains and ML models [23, 24, 25, 26]. The large majority of the papers referred to in these surveys target classification tasks on images or text data. Since our aim is not to conduct a survey, we have selected representative statistical and logic-based approaches, suitable for tabular data. In particular, we chose methods based on feature attribution. These methods are particularly effective in models where understanding the influence of specific inputs is crucial [24].

Existing statistical techniques, notably SHapley Additive exPlanations (SHAP) [27], have become a de facto standard for model interpretability by quantifying the contribution of each feature present in a prediction. However, recent studies [28, 29, 30] highlight potential shortcomings in the theoretical foundation of statistical methods. We are interested in understanding whether SHAP’s reliance on approximate Shapley values can yield misleading

explanations, particularly by failing to capture meaningful relationships between input samples and features appearing in alerts. In cybersecurity, such inaccuracies are critical, as flawed explanations can lead to missed causes, or delayed, ineffective, and even harmful responses.

Logic-based explainability methods [28], and in particular those operating on tree ensembles, such as VoTE-XAI [31], have been proposed to provide minimal, provably correct explanations. Since logic-based explanations are known to have polynomial-time complexity in the size of the model [32, 33], it is interesting to assess whether they are useful in a high-dimensional domain like 5G networking. Given that network outages have been shown to last over a day², we believe that studying the capabilities of such methods towards rapid root-cause identification and service restoration is worth attention. Yet, the potential of logic-based explainability in live incident response remains largely unexplored.

The contribution of this paper is two-fold.

1. We thoroughly analyze the merits of logic-based and statistical interpretations of alerts based on feature attribution, with data from three different 5G testbeds, focusing on conciseness and stability across multiple samples. In particular, we:
 - show the conciseness of the minimal explanations by VoTE-XAI even in high-dimensional settings,
 - identify instability in SHAP’s feature attribution compared to VoTE-XAI,
 - illustrate divergence among the methods in terms of attack-specific features consistently captured by VoTE-XAI but overlooked by SHAP.
2. Trade-off analysis between explainability and computational efficiency in the 5G context. Specifically, we:
 - compare runtime performance, showing VoTE-XAI yields faster single (minimal) explanation outputs,
 - quantify the cost of generating *all* minimal explanations, potentially useful in a forensic analysis.

²<https://www.vodafone.pt/en/press-releases/2022/2/cyberattack-on-vodafone-portugal.html>

The remainder of the paper is organized as follows: Section 2 provides an overview of the feature attribution methods applied in the paper; Section 3 shows the proposed workflow, while Section 4 provides details regarding the use cases. The evaluation criteria are shown in Section 5, and the results are detailed in Section 6. The outcomes, threats to validity, and future directions are discussed in Section 7. Section 8 reviews the related work. Finally, Section 9 ends the paper with closing remarks.

2. Background

XAI refers to a suite of techniques that aim to enhance transparency and improve user trust in ML models by adding accountability to their decision-making processes and providing insights into how predictions are generated. The need for explainability was recognized long before the term XAI was introduced in 2016, with early works already highlighting challenges in making model reasoning accessible to end users [34].

Although there is no general agreement on how explainability shall be understood, the methods can be classified along multiple dimensions, including the scope of explanation, the stage of application, and the dependency on model architecture [35, 25]. For instance, global explanations offer insights into the overall decision-making behavior of an ML model, while local explanations focus on individual outputs. Another classification considers whether a technique depends on a model’s internal structure. Model-agnostic methods explain predictions using only inputs and outputs. Model-specific methods, in contrast, leverage the internal mechanisms of particular ML architectures.

In this research, we apply two explainability techniques for local explanations: SHAP, which estimates feature importance using statistical approaches, and for which we rely on the TreeExplainer optimization³, and VoTE-XAI, a logic-based explanation technique designed for tree ensembles.

2.1. SHAP

SHAP is an explainability technique grounded in cooperative game theory. It explains individual predictions by assigning importance scores, known as Shapley values, to input features. These scores represent the contribution of each feature to the model’s output.

³<https://shap.readthedocs.io/en/latest/generated/shap.TreeExplainer.html>

The Shapley value ϕ_i , for a feature i is defined as shown in Equation 1:

$$\phi_i = \sum_{S \subseteq F \setminus \{i\}} \frac{|S|!, (|F| - |S| - 1)!}{|F|!} [f_{S \cup \{i\}}(x_{S \cup \{i\}}) - f_S(x_S)] \quad (1)$$

Where F is the set of all features, $S \subseteq F \setminus \{i\}$ is a subset of features excluding i , $f_{S \cup \{i\}}$ is the model trained with features in $S \cup \{i\}$, while f_S is the model trained with only features in S . Finally, $x_{S \cup \{i\}}$ and x_S are the input values for the respective feature subsets.

SHAP is generally model-agnostic, as it can be applied to a wide range of ML models. However, optimized implementations exist for specific architectures, such as the TreeExplainer module for tree ensembles. This method is widely adopted due to its scalability and ability to provide both global and local explanations of model behavior.

2.2. VoTE-XAI

VoTE-XAI focuses on generating explanations for predictions made by tree ensemble models. The approach provides explanations that are provably correct and minimal with respect to a given prediction inferred from the model. Specifically, an explanation E is valid for a prediction $f(c_1, \dots, c_n) \mapsto d$ if:

$$\bigwedge_{(x_i, c_i) \in E} (x_i = c_i) \implies f(x_1, \dots, x_n) = d \quad (2)$$

Where x_1, \dots, x_n are the features, c_1, \dots, c_n are their respective values, and d is the model’s prediction. An explanation E is minimal if removing any element from E invalidates the explanation. The formal definition is provided in Equation 3:

$$\forall A \subset E, \bigwedge_{(x_i, c_i) \in A} (x_i = c_i) \not\Rightarrow f(x_1, \dots, x_n) = d \quad (3)$$

VoTE-XAI starts with a full explanation consisting of all feature-value pairs involved in a prediction. It then applies a deletion filter that iteratively removes features. An abstract interpretation-based oracle efficiently checks whether each reduced explanation still leads to the same prediction. If so, the feature is discarded. Otherwise, it is kept in the minimal set.

3. Investigating Feature Attribution for 5G Attacks

This study investigates the effectiveness of the above two representative methods in the context of 5G security monitoring. We conjecture that logic-based explanations, such as those provided by VoTE-XAI, offer a more concise, stable, and computationally efficient representation of feature contributions to classifier alerts (referred to as predictions above). This is particularly critical for real-time security applications, where delayed, overly verbose, or misleading explanations can hinder effective threat mitigation and timely response.

3.1. Research Questions

To test our initial conjecture, we define the following research questions:

- RQ1: How do statistical (SHAP) and logic-based (VoTE-XAI) approaches differ in identifying and prioritizing critical features relevant for intrusion detection alerts across different 5G security scenarios?
- RQ2: What are the computational efficiency trade-offs between SHAP and VoTE-XAI in generating explanations, and how do these trade-offs impact real-time 5G security monitoring?

3.2. Investigation Approach

The workflow is summarized in Figure 1. It consists of four steps which are further detailed in Section 5:

1. **Raising alerts with Trained Model:** An XGBoost classifier is trained and used to generate alerts on the test data. The model’s classification output serves as the input for subsequent explainability analysis.
2. **Selection of True Positives for Explanation:** Only true positive (TP) malicious flows are selected for explanation, ensuring the analysis focuses on correctly identified attacks.
3. **Explanation Generation via Feature Attribution:** For each alert, statistical explanations are derived using SHAP, and logic-based ones are computed using VoTE-XAI.
4. **Analysis:** The resulting explanations are evaluated based on the metrics defined in Section 5. The findings help evaluate the conciseness of the explanations, determine whether the two methods produce contradictory explanations, and assess computational efficiency.

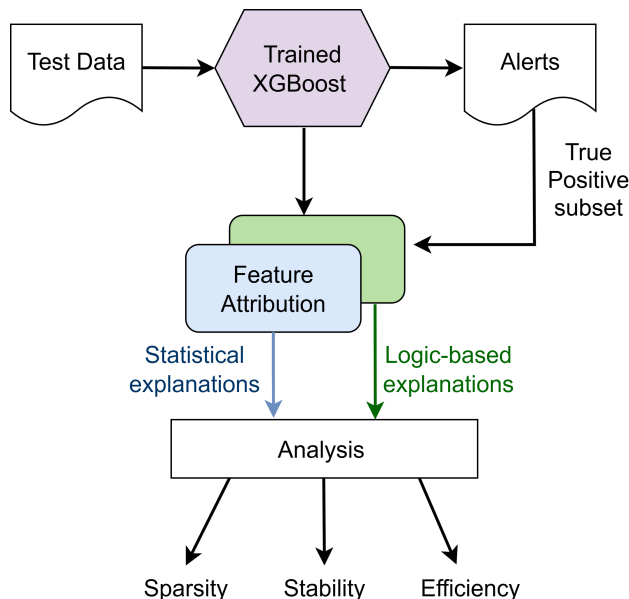


Figure 1: High-level representation of the investigation approach.

4. Incident-response Case Studies

Open datasets for studying 5G network attacks and defenses are few and far between. The existing ones are not ideal due to a severe imbalance in data (benign/attack) categories since they are created in research labs for attack classification or the study of a specific mitigation response. However, our goal here is to create interpretations of alerts raised while monitoring, attributing the attack to identified feature sets. Therefore, potential deficiencies in the datasets will not be relevant for our work, which focuses on the alert level.

This section describes the datasets used and the ML models created for detection of attacks, their training configurations, and performance.

4.1. Dataset Description

We use three available datasets for studying 5G attacks: the 5G Network Intrusion Detection (5G-NIDD) [36], Multistep Attack (MSA) [37], and Packet Forwarding Control Protocol (PFCP) [38] datasets. Although we could have applied our approach to better-known but not 5G-related network intrusion detection benchmarks, we observe that those datasets are rather low-dimensional relative to the complexities in 5G networks reflected in terms of the number of features. For instance, CICIoT2023 [39] and CIC

UNSW-NB15 [40] contain 46 and 76 features, respectively, which is fewer than even our use case with the lowest dimension in the next subsections. The details of the datasets adopted are in the following, and summarized in Table 1.

4.1.1. 5G-NIDD

The 5G-NIDD provides labeled network traffic data, distinguishing between normal operations and attack scenarios. It includes 92 network flow features, such as flow duration, packet size statistics, protocol types, flow flags, and packet inter-arrival times.

The dataset supports both binary and multiclass classification for intrusion detection, and it includes two primary attack categories:

- Denial of Service (DoS): Includes volumetric (ICMP Flood, UDP Flood), protocol-based (SYN Flood), and application-layer attacks (HTTP Flood, Slowrate DoS).
- Port Scans: Comprising SYN Scan, TCP Connect Scan, and UDP Scan.

In total, the dataset comprises 1,215,890 network flows, with 477,737 benign flows (39.29%) and 738,153 malicious flows (60.71%). In this study, the flows were split into training and test subsets using an 80:20 ratio, with 95,833 benign flows and 147,341 malicious ones from the 8 categories above in the test set.

The original documentation was not complete in terms of explaining the features of the data set. Thus, additional work was needed to understand the meaning of the feature names referred to. These are useful for understanding the rest of this paper (Appendix A).

4.1.2. MSA Dataset

The MSA dataset includes labeled data representing a wide variety of attacks on the control plane of 4G/5G networks. It was selected to evaluate the scalability of explanation methods, given its high dimensionality in terms of features (478 in total).

The dataset includes 25,160 samples, 905 benign (3.58%) and 24,255 malicious (96.42%), for a total of 21 distinct types of attacks, classified in 4 categories. Some of the attacks are significantly underrepresented in the

dataset, which can limit their usefulness for training and evaluation purposes. Therefore, we selected the following subset of attacks to include all the categories:

- DoS: Includes several variants, such as “NAS counter Desynch attack”, “Authentication relay attack”, “Handover hijacking”, “RRC replay attack”, “Incarceration with rrcReestablishReject”.
- Bidding Down Attacks: These attacks aim to downgrade the network capabilities of the User Equipment (UE) by exploiting vulnerabilities in unprotected signaling messages. The selected attacks include bidding down with AttachReject and with TAURreject. Applying this attack to a set of UEs would amount to a regional outage scenario.
- Location Tracking: Represented by the Location tracking via measurement reports attack, where the attacker leverages the control plane to extract detailed location information from victim UEs.
- Battery Drain: These attacks force excessive signaling, state transitions, or repeated cryptographic operations, resulting in rapid energy depletion in (a set of) UEs.

We applied an 80:20 train/test split to the dataset. Our subset of the dataset used for tests includes 4,846 malicious and 186 benign flows.

4.1.3. PFCP Dataset

The focus of this dataset is the security issues of the Packet Forwarding Control Protocol (PFCP), which is used in the N4 interface between the Session Management Function (SMF) and the User Plane Function (UPF) in the 5G core. The dataset comprises a total of 83 network features and 7,199 labeled flows, with 1439 normal (20%) and 5760 malicious ones (80%), evenly distributed across the attack classes.

The malicious flows correspond to the following attack scenarios:

- PFCP Session Establishment DoS Attack: Flooding the UPF with legitimate session establishment requests to exhaust its processing capacity.
- PFCP Session Deletion Flood: Overwhelming the UPF with session deletion requests, forcing disconnection of UEs from their active data sessions.

Table 1: Summary of datasets’ dimensionality, balance (ratio of benign and attack records), and attack types.

Dataset	# Features	Total Samples	Benign	Malicious	# Attack Types
5G-NIDD [36]	92	1,215,890	477,737 (39.3%)	738,153 (60.7%)	8
MSA [37]	478	25,160	905 (3.6%)	24,255 (96.4%)	21
PFCP [38]	83	7,199	1,439 (20%)	5,760 (80%)	4

- PFCP Session Modification Flood (DROP): Injecting modifications to Forwarding Action Rules (FAR) that apply the DROP action, resulting in packet discarding for affected sessions. While this disconnects the UE from the Data Network (DN), the UE remains connected to the 5G core via the Radio Access Network (RAN).
- PFCP Session Modification Flood (DUPL): Duplicating session rules to create multiple possible forwarding paths for identical traffic, leading to potential packet duplication and unexpected network behavior. At scale, this attack can cause a distributed DoS across multiple UEs.

Following the same methodology as for the other datasets, we applied an 80:20 train/test split. The resulting test set contains 411 benign flows and 1,646 malicious flows. The features are described in detail in the dataset documentation [38].

4.2. Machine Learning Model

For classification of the attacks, we tested three different tree ensemble models: XGBoost, Random Forest, and LightGBM, with very similar results in terms of detection performance.

Then, the XGBoost Classifier was selected due to its ability to handle class imbalance effectively using the `scale_pos_weight` parameter and to prevent overfitting via regularization techniques inherent to its algorithm. Additionally, there is evidence of its suitability for network intrusion detection tasks and high scalability [41].

Hyperparameter tuning was performed using `RandomizedSearchCV` from the `scikit-learn` library. The model was configured with the hyperparameters outlined in Appendix B, selected based on the results of the `RandomizedSearchCV` optimization process. The selection of alerts to explain is based on binary classification, but multiclass labels are retained for later steps.

The XGBoost model was evaluated on the selected datasets (Step 1 in the workflow from Section 3.2). As shown in Table 2, the metrics used

include True Negatives (TN), False Positives (FP), False Negatives (FN), TP, Accuracy, Precision, Recall, and F1-score⁴. Note that the perfect recall in the PFCP Dataset is likely the consequence of the small size of the original dataset.

To get an idea about the set of alerts that can be subject to explanation, the number of samples in each category in Table 2 is useful. Recall that our goal was not to develop the best possible detector, and the table is only to provide information about the test environment for the explanation study in the next section.

4.3. Alert Selection

Our experiments with explainability (Section 5) took the test set, selecting malicious samples in a stratified manner across all attack classes (Step 2 in the workflow). That is, we identified the indices of samples classified as malicious and retrieved their corresponding attack class labels.

Only samples recognized as TP were selected. This was done to ensure the set subject to explainability contained only attacks that were detected and correctly classified, so that any insights gained from the explanations could be related to the attack characteristics during validation. We realize that, to an operator, both TPs and FPs need explanations. As seen in Table 2, the number of FPs is very low. However, we examined explanations for all FP cases in the 5G-NIDD dataset. The goal was to find out whether explanations might aid in discerning classification errors in some way. Details are provided in Appendix C. FNs result in missed threats, therefore never investigated by the operator. If of any use, explanations of such instances can only help at a pre-operational stage to investigate the quality of the model, which falls beyond our present scope.

Before performing the explainability analysis, we need to select TPs among the possible ones. While selecting, we performed stratified sampling to ensure a balanced selection across attack types, allocating an equal number of samples per class, aiming to keep the total TPs below 100. This number was selected so that the validation of all explanations manually would be feasible.

More specifically, for each attack class, we first identified all malicious samples belonging to that class and performed stratified sampling without

⁴Definition of these metrics is standard but can be found in the Scikit-learn user guide: https://scikit-learn.org/stable/modules/model_evaluation.html

replacement. This means that once a sample is selected, it is not chosen again. However, replacement was incorporated as a fallback mechanism to ensure that if a particular class had fewer samples than required, additional instances could be drawn to maintain balance.

The final sets adopted for the explainability experiments consisted of 88 samples for the 5G-NIDD dataset (11 per attack class), 80 samples for the MSA dataset (8 per attack class), and 100 samples for the PFCP dataset (25 per attack class).

Table 2: Confusion matrix elements and evaluation metrics for the XGBoost Classifier for both datasets.

Dataset	TN	FN	FP	TP	Accuracy	Precision	Recall	F1-Score
5G-NIDD	95796	35	37	147306	0.9997	0.9997	0.9998	0.9997
MSA	152	4	34	4842	0.9924	0.9930	0.9992	0.9951
PFCP	409	0	2	1646	0.9990	0.9988	1.0000	0.9994

5. Experiment Design and Evaluation Strategy

This section outlines the experimental approach. The results are shown in Section 6. The source code and data used in this study are available on GitHub⁵. This repository will be made public upon paper acceptance.

5.1. Evaluation Metrics

The field of XAI has seen a proliferation of evaluation metrics, with no universally accepted standard, [42]. Hence, to evaluate the performance of both statistical and logic-based approaches, we adopted three metrics: sparsity, stability, and efficiency, drawing on definitions from Warnecke et al. [43] (for sparsity and efficiency), and from Alvarez-Melis and Jaakkola ([44] for stability).

Sparsity: An explanation is considered meaningful if it involves only a limited number of features. It can be considered the opposite of verbosity. This type of interpretability measure is intended to reduce the cognitive load for analysts in a human-in-the-loop scenario. Thus, we evaluate how concise the explanations are in highlighting the most relevant features.

⁵Source Code: <https://github.com/FedeU95/5GXAI>

Stability: Stability is a widely discussed but not universally agreed-upon metric in XAI. It can be defined as the consistency of an explanation method when applied to similar input instances. In this study, stability refers to the degree to which explanations remain similar within alert samples from the *same* attack class.

Efficiency: An explanation method is deemed efficient if it can be considered plausible in an operational workflow. Real-world threat detection scenarios, such as those in 5G networks, require explanations that are not only accurate and interpretable but also timely (a notion that we will discuss in Section 6.4).

5.2. Analysis of Sparsity and Stability

This analysis examines how concise SHAP and VoTE-XAI explanations are (using sparsity) and whether they remain consistent within the same attack class (using stability).

If explanations vary significantly within the same class, it might indicate the inability to generate consistent explanations. Consistent explanations across samples and attack classes suggest a method is more trustworthy for security analysts when diagnosing root causes.

By comparing VoTE-XAI’s logic-based selected features with SHAP’s statistical attributions on the same alert (class), we assess the alignment of statistical and logic-based explanations in a 5G scenario. We ran all the test data flows from each dataset as mentioned in Section 4.3 with the trained attack classification model. Then, both explanation approaches were applied to the subset of the true positive instances the model identified.

For SHAP, we employ the TreeExplainer module. Explanations are computed by selecting all the features with positive attribution, resulting in one individual explanation per sample. Note that a very low SHAP value in that approach signifies a small likelihood of the relevance of a feature, but we chose to include all such features so that no explanations would be missed due to choosing an arbitrary threshold. In the context of our study, features with negative SHAP values are not considered relevant, as they represent factors that did not contribute to the raising of that alert. Hence, the potential usefulness of these falls outside the scope of our analysis.

We assess the stability of feature attribution within each attack class by computing the minimum, maximum, and mean SHAP values per feature. This helps identify how consistently SHAP associates importance to specific features across different samples of the same attack class. It also shows

whether certain features dominate explanations or if feature attributions fluctuate widely. By comparing SHAP distributions within each attack class, we assess feature stability (consistent attribution) vs. variability (fluctuating importance across samples from the same attack type).

VoTE-XAI is evaluated by identifying features that appear consistently across all minimal explanations for each sample of each attack type. Note that, unlike SHAP, which assigns importance scores based on statistical contributions, VoTE-XAI provides logic-based, minimal explanations that highlight the logically valid features for a given classification. There may be different minimal explanations for the same alert, but they are all valid explanations. The method also allows calculation of all minimal explanations for a given alert.

To get an idea about variations among those, all minimal explanations were computed for each sample and attack class. The features were ranked based on their occurrence across all minimal explanations.

5.3. Divergence Among the Methods

The degree of alignment between SHAP and VoTE-XAI feature attributions relates to RQ1 in Section 3, and is investigated by comparing the features according to SHAP’s top-ranked feature importance values with the most frequently occurring features in VoTE-XAI minimal explanations for each attack class.

A high agreement between these methods suggests that SHAP’s statistical attributions align with VoTE-XAI’s logic-based explanations. Conversely, low agreement indicates a divergence between the methods. Given that VoTE-XAI provides logically sound attributions, this suggests that SHAP may introduce misleading outputs, potentially complicating the security analyst’s task rather than aiding it.

5.4. Runtime Performance Evaluation

The purpose of this analysis is to evaluate the efficiency of SHAP and VoTE-XAI (relating to RQ2) by measuring the time required to generate explanations. Real-time threat detection in 5G networks requires fast and interpretable explanations to support immediate decision-making. If an explainability method is computationally expensive, it risks becoming impractical for deployment in security operations. However, slower methods can still be useful in forensic contexts.

The analysis is based on a large TP alert set consisting of 1,200 samples, selected using the same procedure described in Section 4.2.

6. Evaluation Outcomes

This section presents the experimental results, aiming to answer RQ1 (Subsections 6.1, 6.2, and 6.3) and RQ2 (Subsection 6.4) following Steps 3 and 4 of the workflow described in Section 3.2.

6.1. Sparsity Evaluation

SHAP assigns an importance score to each feature, indicating its contribution to the model’s output. On average, it is observed that SHAP explanations are consistently more verbose than VoTE-XAI’s ones across the three use cases.

Specifically, each SHAP explanation includes 20–25 features with positive attributions out of the original 92 in use case 1 (5G-NIDD). For use case 2 (MSA), SHAP explanations identify between 59 and 90 features per sample, among the 478 from the full set. For use case 3 (PFCP), each SHAP explanation includes 16-20 features out of the original 83.

When computing only one minimal explanation for each sample, it is observed that VoTE-XAI provides more concise (less verbose) explanations compared to SHAP. For use case 1 (5G-NIDD), 6-15 features were identified on average. In use case 2 (MSA), explanations contain 27–41 features out of the 478 in the original dataset, less than half the size of SHAP’s output. For use case 3 (PFCP), each VoTE-XAI explanation consists of only 4–6 features.

6.2. Stability Evaluation

In all the use cases, SHAP values fluctuate significantly across different samples of the same attack class. This highlights a possible limitation of statistical XAI: its attributions may be unstable for specific cases, potentially leading to misleading interpretations. In contrast, VoTE-XAI provides highly consistent explanations across samples: features identified as critical by VoTE-XAI appear in nearly every explanation for a given attack class. More details are in Appendix D.

Figure 2 presents the five features with the highest mean SHAP values for given attack classes (x-axis). For each feature, the blue bar shows the mean SHAP value across all samples of that attack class (y-axis). The markers above and below the bar denote the maximum and minimum SHAP values

observed for that feature, thereby indicating the variability of attributions. Low variability implicitly indicates more reliable attribution.

Considering the stability of SHAP in the three use cases, we see that SHAP values range from 0 to 8.28 for 5G-NIDD. For UDPFlood (Figure 2a), *Seq* and *Offset* hold the highest importance with moderate variability, while protocol-specific features (e.g., *udp*) are less relevant. In DoS attacks (e.g. SYNflood, Figure 2b), SHAP shows high variance, often overestimating feature importance, whereas scan-based attacks yield lower variability.

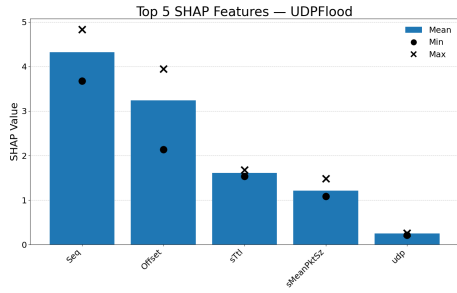
For the MSA use case, SHAP values range from 0 to 2.91. Variability is greater than in 5G-NIDD: in both “Bidding down with TAUREject” (Figure 2c) and “Authentication relay attack” (Figure 2d), features often receive zero attribution for some instances but higher attribution for others, reflecting low stability. In these and the following charts, the features from this dataset are indicated as F1,..., F25 for readability. Their full feature names and description appear in Table 4 (Appendix A).

SHAP values range from 0 to 1.17 for the PFCP use case. Explanations again show considerable variability: in the Session Deletion Flood (Figure 2e), *Fwd IAT Min* is most important, while *Dst IP* and *Fwd Pkts/s* fluctuate; in the Modification Flood (DROP) (Figure 2f), *Fwd IAT Min* and *Dst Port* are unstable.

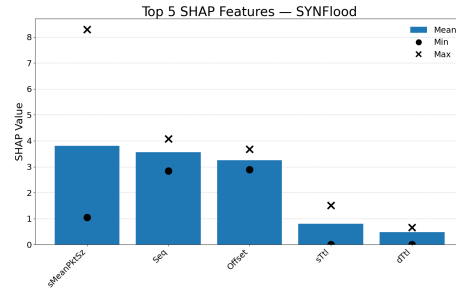
The heatmaps in Figure 3 visualize the stability of VoTE-XAI explanations across the three datasets by highlighting recurring feature patterns within each attack type. The x-axis refers to the attack classes, while the y-axis shows the features. The cells represent the occurrence (in %) of the features across the explanations of all samples for the given attack type. Darker cells indicate features that appear with higher frequency.

In 5G-NIDD, VoTE-XAI highlights a consistent core of features per attack class for all minimal explanations per sample (Figure 3a). Some features consistently appear in over 80% of the explanations across multiple attack types, indicating their high relevance in distinguishing malicious activity (e.g. *Seq*, *sTtl*, *Offset*). Certain features appear consistently in specific attack types, reflecting their attack-class dependence (e.g. *ECO* has near-perfect frequency only for SlowrateDoS and HTTPFlood).

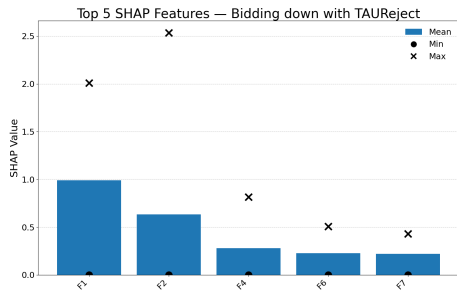
For the MSA dataset, with the 478 dimensional model, the numbers on charts are based on the calculation of all minimal explanations found by VoTE-XAI with a 1 hour timeout. As shown in Figure 3b, VoTE-XAI maintains high intra-class consistency, distinguishing globally relevant features (indicative of protocol-level malicious behavior) from those specific to indi-



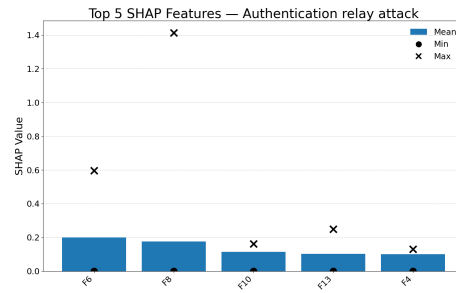
(a) UDPFlood



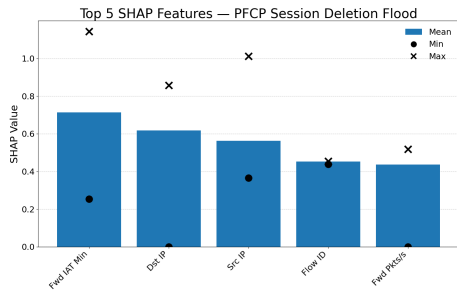
(b) SYNflood



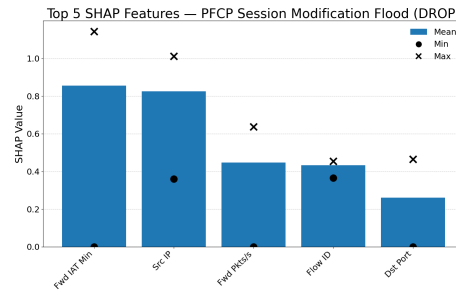
(c) Bidding down with TAUREject



(d) Authentication relay attack



(e) PFCP Session Deletion Flood



(f) PFCP Session Modification Flood (DROP)

Figure 2: SHAP stability across different attacks: (a) UDPFlood, (b) SYNflood, (c) Bidding down with TAUREject, (d) Authentication relay attack, (e) PFCP Session Deletion Flood, (f) PFCP Session Modification Flood (DROP).

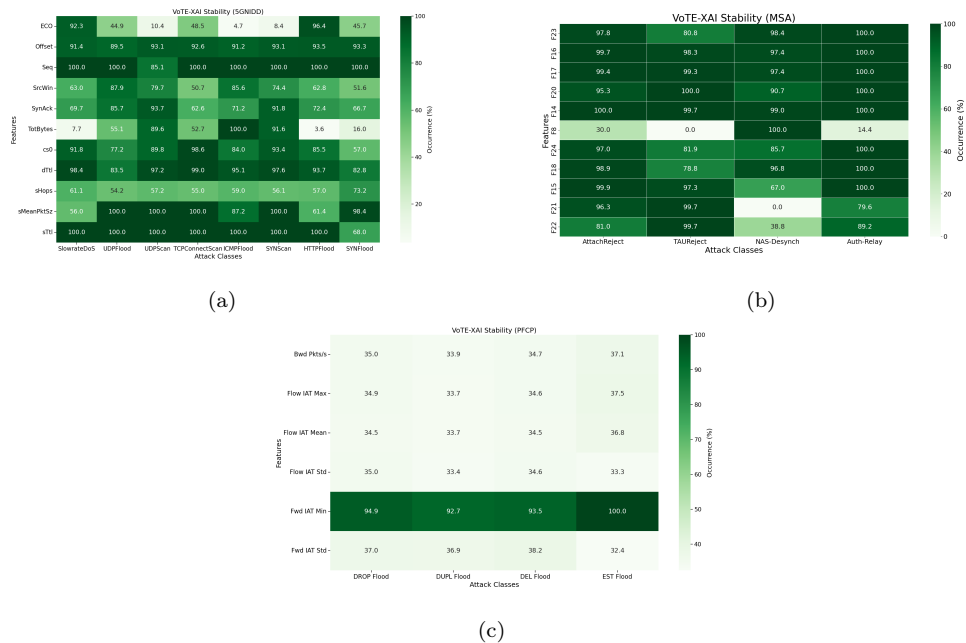


Figure 3: VoTE-XAI stability for (a) 5G-NIDD, (b) MSA, and (c) PFCP datasets.

vidual attack types. For conciseness, the heatmap for this use case shows a subset of four representative attacks out of the full set of ten.

In the PFCP use case, VoTE-XAI explanations show a high degree of stability, calculated based on all minimal explanations per sample: all four attack types share a near-identical core set of features, with negligible differences in terms of occurrence for DROP and DUPL attacks (Figure 3c). This consistency is expected, as the underlying traffic characteristics of PFCP floods are similar across variants.

6.3. Divergence Among the Methods

The results in the last subsection reveal significant divergence between SHAP and VoTE-XAI. Several features that appear in over 80% of VoTE-XAI explanations have low or zero SHAP attribution, indicating a fundamental misalignment between the methods.

Figure 4 highlights representative cases where VoTE-XAI and SHAP exhibit significant discrepancies in feature attribution. In the charts, the green y-axis represents VoTE-XAI occurrence (in %), while the blue one represents the mean SHAP values. The x-axis shows the features most frequently

selected by VoTE-XAI (occurrence $>80\%$; for the PFCP dataset, a lower threshold of 30% was used for visualization). It is worth mentioning that a similar trend was observed in each attack class, with SHAP systematically assigning near-zero scores to at least one of the top VoTE-XAI features.

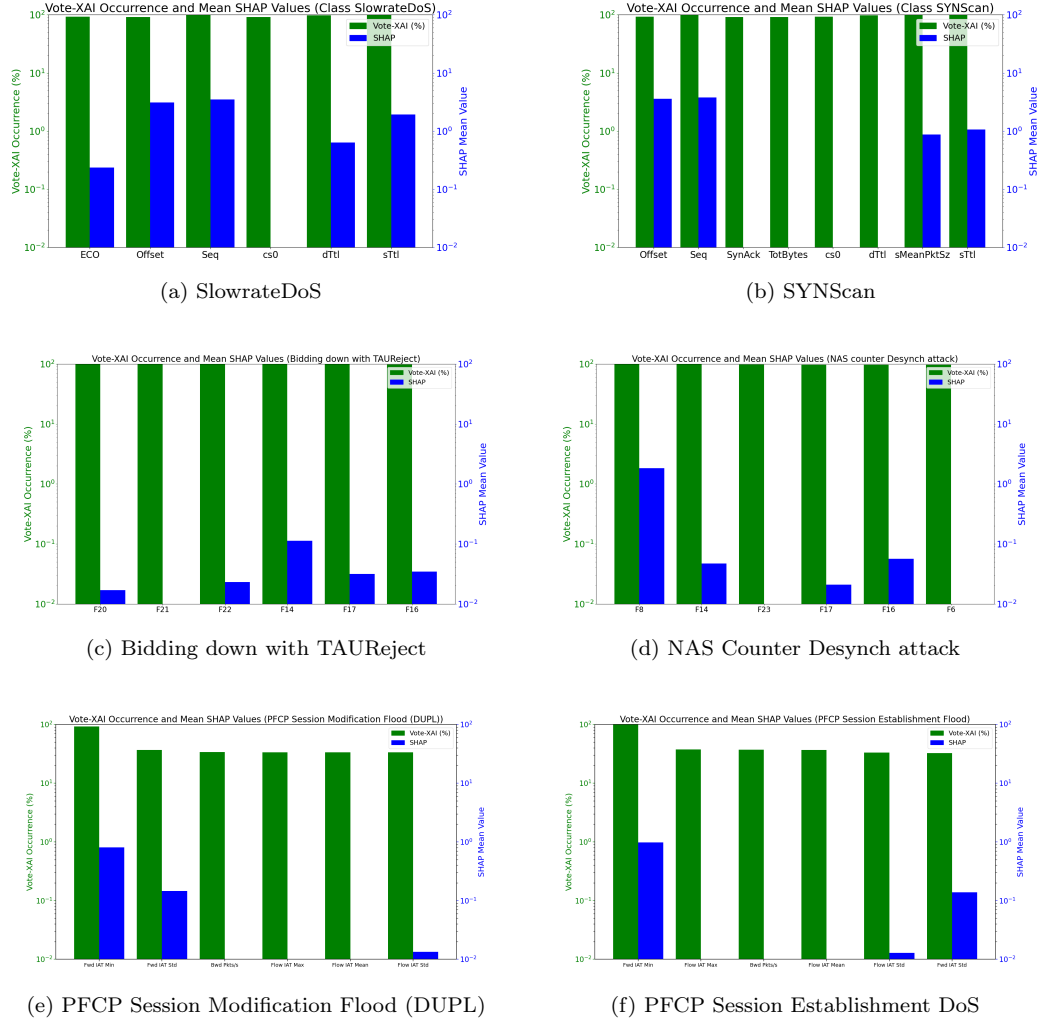


Figure 4: Divergence between VoTE-XAI feature importance (green bars) and SHAP attribution (blue bars) across six attack types. The y-axes are in logarithmic scale.

5G-NIDD. In SlowrateDoS (Figure 4a), features such as *dTtl* (occurrence 98.4%) and *ECO* (92.3%) are consistently selected by VoTE-XAI but underestimated by SHAP (0 and 0.24, respectively), despite being critical

indicators of slow-rate attacks. In SYNScan (Figure 4b), VoTE-XAI highlights *dTtl* (97%) and *TotBytes* (91.6%), while SHAP again assigns them zero importance. This raises concerns about SHAP’s ability to detect subtle TCP scan indicators, which often exploit TTL behavior and byte patterns in network interactions.

MSA. Similar discrepancies appear in signaling-centric and identity manipulation attacks. For instance, in “Bidding down with TAUREject” (Figure 4c) and the “NAS counter Desynch attack” (Figure 4d), VoTE-XAI consistently selects protocol-level fields (e.g., NAS identifiers, encoding details) with high frequency, while SHAP attributes them near-zero importance. Comparable patterns are observed in other MSA attack classes.

PFCP. Disagreements are also evident in this use case. For PFCP Session Modification Flood (DUPL) (Figure 4e), both methods align on *Fwd IAT Min* (92.7%, SHAP: 0.81), but diverge on others: VoTE-XAI highlights *Bwd Pkts/s* (33.9%, SHAP: 0.0023) and *Flow IAT Max* (33.7%, SHAP: 0.0009). In Session Establishment DoS (Figure 4f), VoTE-XAI consistently emphasizes *Flow IAT Max* and *Bwd Pkts/s*, both overlooked by SHAP. Similar trends hold across other PFCP floods.

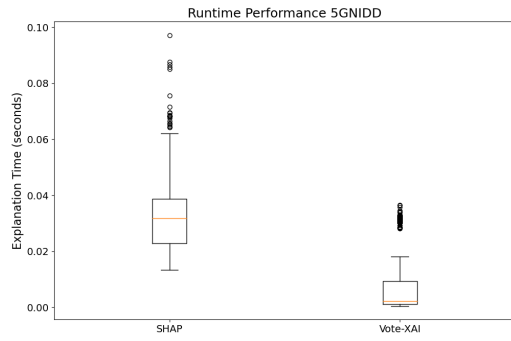
These results confirm our intuition that logic-based explanations are not only less verbose but also consistent within an attack class. They also answer RQ1 by systematically identifying the divergent behaviors of the two approaches on the same model across three use cases. Section 7 provides a deeper discussion.

6.4. Runtime Performance Evaluation

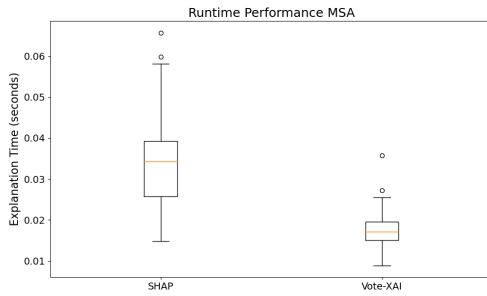
This section evaluates the runtime efficiency of SHAP and VoTE-XAI explanations. The results, shown in Figure 5a, 5b, and 5c, compare the SHAP runtime to the time required to compute one minimal explanation per sample using VoTE-XAI.

For 5G-NIDD, the mean runtime for SHAP is 0.032 seconds, whereas VoTE-XAI demonstrates a significantly lower mean runtime (0.002 seconds). Additionally, the outliers for VoTE-XAI are fewer and lower than the SHAP outliers. This indicates a more stable computational performance. In contrast, SHAP exhibits extreme outliers, with some runtimes reaching up to 0.1 seconds.

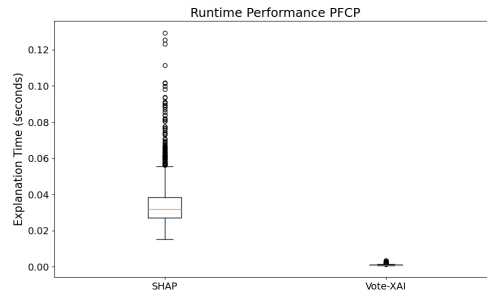
A similar trend is observed in the MSA use case, with a mean runtime of 0.034 seconds for SHAP, and 0.0017 seconds for VoTE-XAI, and in the PFCP one (0.03 seconds for SHAP, and 0.001 seconds for VoTE-XAI). These



(a)



(b)



(c)

Figure 5: Runtime Performance Evaluation for SHAP and VoTE-XAI (single minimal explanation) for the 5G-NIDD (a), MSA (b), and PFCP (c) datasets.

findings confirm that computing one minimal explanation per sample using VoTE-XAI is likely to be faster than SHAP.

However, computing *all* minimal explanations for a single alert is significantly more time-consuming, which we do not show by charts here but only summarize. VoTE-XAI requires between 0.5 and 9 seconds per sample for the 5G-NIDD dataset, and between 0.6 and 1.8 seconds for the PFCP dataset. During this time, hundreds of minimal and provably correct explanations are computed per sample. Note that Figure 4 showed the convergence of the features appearing in those different minimal explanations to a great extent.

For the MSA dataset, given the larger feature space and thereby a much larger search space, the full computation of all minimal explanations for a single attack class required approximately 17 hours on average. Due to this high computational demand, a timeout of one hour was set when computing all minimal for the stability and divergence analyses presented in previous sections. We will discuss this further in Section 7.

7. Discussion

The above experimental results provide some insights regarding trade-offs between statistical and logic-based explainability methods. While SHAP is grounded in a model-agnostic framework, in our case we used its TreeExplainer module, optimized for tree ensembles. This optimization improves computational efficiency and ensures fair allocation of feature contributions, yet the resulting explanations still tend to be less succinct and less informative in this concrete security setting, as we discuss below.

7.1. Sparsity and Efficiency

We saw that VoTE-XAI provides less verbose feature attributions, which is significant for mitigation in systems with large feature sets. Regarding computational efficiency, VoTE-XAI is significantly faster than SHAP, making it suitable for real-time security monitoring.

When asked to calculate *all* minimal explanations for a given alert, the runtime of VoTE-XAI can increase significantly, as shown in the case of the MSA dataset. This highlights a key trade-off: VoTE-XAI is capable of providing a more comprehensive analysis if additional computation time is available, but already with one minimal explanation directs to logically valid explanations, given a model.

In the context of intrusion detection, where real-time response is critical, this trade-off raises an important question: is the added computational cost justified by the additional explanations? Given that DoS attacks can cause significant damage within seconds or minutes [45], further delay might be challenging for immediate mitigation.

On the other hand, for other attacks, and because real network outages can take hours or even days to get sorted out, it may not be an issue to spend the time required to have a full picture (in our use case 1, an additional 9 seconds). While this delay may or may not work in a live detection scenario, it appears plausible in a forensic context. VoTE-XAI’s ability to compute all minimal explanations can definitely enrich post-incident analysis for a more comprehensive understanding of potential causes.

Additionally, instead of all minimal explanations, it would still be possible to compute a limited number of explanations based on time constraints or operational urgency. This hybrid strategy would allow analysts to balance completeness and latency, adapting the explanation granularity to the context.

Incorporating domain expert security knowledge into both methods could further improve the efficiency of explanations. This is already foreseen in the computation engine of VoTE-XAI, which incorporates a cost function for more actionable features (but we ignored by setting all costs to 1 in these experiments). For SHAP values, threshold levels (above zero) would have to be experimentally determined.

7.2. Stability and Correctness

Beyond sparsity and efficiency, a crucial aspect to consider is the reliability of explanations. Reliability rests on stability, meaning that we expect similar explanations over instances of the same attack class.

We saw that VoTE-XAI provides more stable feature attributions, whereas SHAP exhibits higher variability and, in some cases, fails to highlight security-critical features.

Notably, even when VoTE-XAI computes a single (minimal) explanation, the high stability of explanations among attack classes (as seen in Section 6.2) provides some confidence that the security team can act on trustworthy information. This discrepancy raises some concerns about the reliability of SHAP in high-risk applications.

Even with stable explanations, a further concern is correctness. In the 5G intrusion context, correctness refers to semantic validity: do the explanations

align with known attack mechanics? As shown in the previous section, several features consistently highlighted by VoTE-XAI but largely ignored by SHAP correspond directly to detection indicators described in recent literature [46]. For example, in SYN-based flooding and scanning, VoTE-XAI highlighted SYN-ACK handshake timing, an indicator recognized in detecting reconnaissance and handshake abuse. Instead, SHAP emphasizes variables with statistical correlation but weaker causal interpretability (e.g., generic byte counts).

Consequences of inaccurate explanations are missed opportunities to pinpoint the cause of an attack or a waste of resources looking for irrelevant mitigation actions.

7.3. Threat to Validity

A key challenge in 5G security research is the lack of large-scale, diverse, and up-to-date datasets specifically curated for intrusion detection. While the 5G-NIDD dataset is one of the most comprehensive available, it has inherent limitations in diversity and volume, particularly regarding protocol-specific threats. While relevant, the focus on Scan and DoS attacks represents a limited subset of potential 5G security threats.

To partially address this limitation, we incorporate the MSA and PFCP datasets, which focus on more sophisticated and protocol-aware control plane attacks, but are much smaller in terms of sample numbers.

As highlighted by Arp et al. [7], ML in security research is prone to several pitfalls that can undermine the generalizability and reliability of results. Specifically, our use of pre-collected datasets exposes us to sampling bias and imbalance. However, since we focus only on explanations, we believe that the lessons learned can be transferred to new collection setups.

Another threat relates to label inaccuracies arising due to reliance on heuristics or imperfect labeling mechanisms, but the impact of that is limited. Our method was demonstrated on true positive alerts, no matter how they are identified.

Our work confirms the need for realistic testbeds to study different attack and defense patterns, and the release of datasets to assess the usefulness and novelty of new AI-related tools in the security toolbox.

7.4. Towards Usability Studies

Several key areas warrant exploration to further enhance the applicability of explainable AI in 5G security. Future research could focus on qualitative

analysis of the methods through usability studies.

We have conducted a preliminary study using a Large Language Model (LLM), ChatGPT⁶, to simulate domain expert interpretation in 5G security. Separate prompts with feature values were used for each method across different attack classes. When prompted with SHAP features, the LLM often misclassified DoS as probing. In contrast, VoTE-XAI’s feature lists led to more accurate recognition of both scans and DoS in most cases.

While LLM outputs cannot replace expert judgment, this limited exercise shows that VoTE-XAI might have potential in highlighting actionable threat indicators. Our ongoing work studies the 5G-specific expert knowledge embedded in LLM for further study.

8. Related Work

Explainability techniques have been applied to intrusion detection systems (IDS) and security monitoring to enhance interpretability and improve trust in ML-based threat detection. A large body of existing studies focus on statistical XAI approaches, particularly SHAP and LIME, with limited exploration of logic-based explainability in cybersecurity. Below, we summarize the most relevant research and position our study within this landscape.

Gaspar et al. [47] explore SHAP and LIME to interpret predictions from Multi-Layer Perceptron (MLP)-based IDSs. This work aims to evaluate the impact of explainability on the accuracy of the classifier. A perturbation analysis was conducted by removing or replacing features based on their importance in SHAP/LIME explanations and observing changes in classification. The study found that, in certain scenarios, relying on the explanations negatively impacted the model’s performance, suggesting potential inconsistencies in the explanations. While this work uncovers possible limitations of LIME and SHAP, it neither explicitly highlights nor addresses them.

Malwade et al. [48] combine SHAP, LIME, and Counterfactual SHAP to enhance interpretability in IoT security. By employing these explainability techniques, the researchers seek to translate model predictions into actionable strategies for attack mitigation. The study primarily focuses on statistical methods without evaluating possible inconsistencies or limitations.

A neurosymbolic approach to IoT security is proposed by Kalutharage et al. [49], integrating autoencoder-based anomaly detection with SHAP expla-

⁶Version GPT-4o

nations and domain knowledge encoded in a knowledge graph. In contrast to our work, the focus is primarily on improving detection and interpretability of alerts.

Choi et al. [50] propose an attack-specific feature analysis framework for intrusion detection in IoT networks. The approach applies feature selection tailored to attack types and uses SHAP to quantify feature importance. Unlike our study, this work is centered on enhancing the detection performance of unsupervised models and autoencoders through XAI-optimized feature selection.

Najibi et al. [51] apply SHAP and LIME to extract the most influential features from deep neural network classifications. The authors use domain knowledge to classify the top features based on their resistance to evasion and retrain the models using only such features. This is accomplished at the cost of degraded performance detection.

Vo et al. [52] use SHAP for dimensionality reduction, with the aim of improving classification performance in various ML models by retraining the models using only the top features. In their experiments, it is noted that relying on SHAP’s attribution leads to performance degradation in certain cases and slight improvement in others.

Drichel et al. [53] used white-box, gradient-based techniques from the iNNvestigate library⁷ to analyze deep learning models trained to reveal bot-net activity through Domain Generation Algorithm (DGA) detection. Their goal is to use explainability to uncover bias in the classifier, showing a degradation of the model’s performance once the bias is removed. While their findings highlight the value of explainability for understanding classifier behavior, their focus is restricted to deep neural networks and the study of DGA.

In the context of 5G and beyond, Basaran et al. [54] propose XAIomaly, an XAI-enhanced anomaly detection framework for 6G networks. They propose a novel explainability method, fastSHAP-C, designed to operate within the O-RAN architecture. While fastSHAP-C improves efficiency, it inherits SHAP’s statistical limitations, which may produce misleading attributions in security-critical settings.

Terra et al. [55] apply global and local explainability techniques to analyze SLA violations in 5G network slicing, validating their results with causal

⁷<https://github.com/albermax/innvestigate>

inference tools. While a diverse set of explainability techniques is applied, the research does not explore logic-based approaches nor focuses on security, leaving a gap in the potential for rigorous and provably correct explanations in critical network applications.

Fiandrino et al. [56] demonstrate that SHAP, when applied out-of-the-box, produces non-intuitive and costly explanations for deep reinforcement learning (DRL) agents in O-RAN systems, as it relies on intermediate representations rather than meaningful inputs. While they propose a graph-based alternative, its scope is limited to network control and does not extend to intrusion detection or broader security monitoring.

Huang and Marques-Silva [29] critically analyze SHAP’s shortcomings in security settings, demonstrating that its assumptions of feature independence can lead to misleading attributions in complex datasets. The authors argue for the development of more reliable explanation methods that accurately reflect feature relevance, but proposing an alternative was not in the scope of their work. This highlights the necessity for alternative explainability methods that do not rely on unrealistic statistical assumptions.

Marques-Silva [33] gave a tutorial in a summer school, highlighting that statistical methods like SHAP and LIME often yield inconsistent and logically unsound explanations using small-scale synthetic models. They suggest that abductive and contrastive explanations, computed via Boolean Satisfiability (SAT) and Maximum Satisfiability (MaxSAT), can ensure rigor and minimality in explanations.

Our work takes this theoretical observation further to evaluate logic-based explainability in a practical landscape, applies it to 5G security, and further studies the timeliness of the explanation computations. Compared to the above state of the art, we empirically evaluate SHAP and VoTE-XAI based on explanation sparsity, stability, and efficiency in three 5G security use cases.

Finally, we position our work compared to the work introducing VoTE-XAI. Törnblom et al. [31] focus on the theoretical underpinnings of the method to derive the explanations in tree ensembles, the soundness and completeness proofs, and some experiments in order to compare the approach to MaxSAT-based approaches. In these experiments, VoTE-XAI showed superior performance. However, the experimental evaluation is limited to common AI benchmarks, with fewer features (ranging from 7 to 60 as the highest dimension).

As far as we are aware, this work is the first to apply logic-based explanations in intrusion detection with a realistic experimental evaluation.

While SHAP and Vote-XAI approaches to explanation are different in nature, we have strived to perform comparative analysis of the meaningfulness and practicality of each on fair grounds.

9. Conclusion

This study evaluated statistical (SHAP) and logic-based (VoTE-XAI) explainability methods for 5G security monitoring. Our findings show that VoTE-XAI consistently identifies critical attack features, whereas SHAP often misattributes importance. VoTE-XAI (logically correct) explanations are also shown to be concise and computationally efficient, making it more suitable for real-time intrusion detection where sub-second calculations suffice.

Note that logically correct in this context means correct with respect to the ML model’s perception of what is an attack and what is benign. Given that ML models are never perfect, we can only come up to the level of accuracy of a model in terms of the relevance of explanations. In other words, given a true positive outcome of a detection, the attributed features by Vote-AI are as correct and accurate as we can get.

For a false positive outcome, the security operator would have to engage in further analysis in any case, and a model with very low false positives is already known to be a critical requirement for any ML model to be useful in the security context, regardless of the explainability method adopted.

Our work illuminates that for run-time analysis, VoTE-XAI is faster than SHAP when generating a single minimal explanation. Computing all explanations incurs additional time, but it will most likely provide additional benefits in a forensic context.

A critical next step is applying the proposed methodology within a realistic testbed environment, where we can control, inject, and monitor traffic in real-time while dynamically analyzing security events. This would enable validation against new classes of relevant attacks, including adaptive ones, and assess the practical viability of VoTE-XAI in active defense scenarios with further mitigation actions.

Integrating explainability into automated security workflows could significantly enhance intrusion response mechanisms. Future work could explore how VoTE-XAI explanations can be leveraged for mitigation, improving analyst decision-making, and reducing response times through user studies. Additionally, the incorporation of expert knowledge or real-time risk assessment to prioritize some (minimal) explanations over others could be further

studied.

Counterfactual explanations provide insights into how a classification decision could change given minimal modifications to input features. In the context of a 5G testbed, counterfactuals could help understand attack evolution. This is a topic we are currently pursuing further. By modifying key network attributes, we could infer how an attacker might evade detection, aiding in proactive defense. Evaluating the impact of adversarial perturbations can also help identify model weaknesses and enhance resilience against stealthy attacks.

Acknowledgment

This work was carried out within the NEST project *AIR*², which is partially supported by the Wallenberg AI, Autonomous Systems and Software Program (WASP) funded by the Knut and Alice Wallenberg Foundation. It was also supported by ELLIIT, the Excellence Center at Linköping – Lund in Information Technology. The authors would like to thank Elisa Bertino and Kazi Samin Mubasshir for collecting the MSA dataset and for providing valuable information during the project.

References

- [1] P. Benlloch-Caballero, Q. Wang, J. M. A. Calero, Distributed dual-layer autonomous closed loops for self-protection of 5G/6G IoT networks from distributed denial of service attacks, *Computer Networks* 222 (2023) 109526.
- [2] G. Apruzzese, P. Laskov, E. Montes de Oca, W. Mallouli, L. Brdalo Rapa, A. V. Grammatopoulos, F. Di Franco, The role of machine learning in cybersecurity, *Digital Threats: Research and Practice* 4 (1) (2023) 1–38.
- [3] M. E. Morocho-Cayamcela, H. Lee, W. Lim, Machine learning for 5G/B5G mobile and wireless communications: Potential, limitations, and future directions, *IEEE access* 7 (2019) 137184–137206.
- [4] L. A. Garrido, A. Dalgkitsis, G. Famitafreshi, A. Siokis, K. Ramantas, C. Verikoukis, An experimental platform of a beyond-5G network with machine learning integration, in: *GLOBECOM 2023-2023 IEEE Global Communications Conference*, IEEE, 2023, pp. 62–67.

- [5] U. K. Lilhore, S. Dalal, S. Simaiya, A cognitive security framework for detecting intrusions in IoT and 5G utilizing deep learning, *Computers & Security* 136 (2024) 103560.
- [6] C.-Y. Lin, S. Nadjm-Tehrani, Protocol study and anomaly detection for server-driven traffic in scada networks, *International Journal of Critical Infrastructure Protection* 42 (2023) 100612.
- [7] D. Arp, E. Quiring, F. Pendlebury, A. Warnecke, F. Pierazzi, C. Wressnegger, L. Cavallaro, K. Rieck, Pitfalls in machine learning for computer security, *Communications of the ACM* 67 (11) (2024) 104–112.
- [8] E. U. A. for Cybersecurity (ENISA), Cybersecurity of AI and standardisation, accessed: Nov. 27, 2024 (2023).
URL <https://www.enisa.europa.eu/publications/cybersecurity-of-ai-and-standardisation>
- [9] P. J. Phillips, C. Hahn, P. Fontana, A. Yates, K. K. Greene, D. Broniatowski, M. A. Przybocki, Four principles of explainable artificial intelligence (2021-09-29 04:09:00 2021).
doi:<https://doi.org/10.6028/NIST.IR.8312>.
URL https://tsapps.nist.gov/publication/get_pdf.cfm?pub_id=933399
- [10] V. Hassija, V. Chamola, A. Mahapatra, A. Singal, D. Goel, K. Huang, S. Scardapane, I. Spinelli, M. Mahmud, A. Hussain, Interpreting black-box models: a review on explainable artificial intelligence, *Cognitive Computation* 16 (1) (2024) 45–74.
- [11] W. Saeed, C. Omlin, Explainable AI (XAI): A systematic meta-survey of current challenges and future opportunities, *Knowledge-Based Systems* 263 (2023) 110273.
- [12] N. Papernot, P. McDaniel, Deep k-nearest neighbors: Towards confident, interpretable and robust deep learning, *arXiv preprint arXiv:1803.04765* (2018).
- [13] H. Shin, J. Choi, D. Lee, K. Kim, Y. Lee, Fully homomorphic training and inference on binary decision tree and random forest, in: *European Symposium on Research in Computer Security*, Springer, 2024, pp. 217–237.

- [14] B. Chander, C. John, L. Warriar, K. Gopalakrishnan, Toward trustworthy artificial intelligence (tai) in the context of explainability and robustness, *ACM Computing Surveys* 57 (6) (2025) 1–49.
- [15] R. Shwartz-Ziv, A. Armon, Tabular data: Deep learning is not all you need, *Information Fusion* 81 (2022) 84–90.
- [16] Q. Zou, L. Zhang, X. Sun, A. Singhal, P. Liu, Using explainable AI for neural network-based network attack detection, *Computer* 57 (5) (2024) 78–85.
- [17] B. Brik, H. Chergui, L. Zanzi, F. Devoti, A. Ksentini, M. S. Siddiqui, X. Costa-Pérez, C. Verikoukis, Explainable AI in 6G O-RAN: A tutorial and survey on architecture, use cases, challenges, and future research, *IEEE Communications Surveys & Tutorials* (2024) 1–1doi:10.1109/COMST.2024.3510543.
- [18] M. T. Ribeiro, S. Singh, C. Guestrin, Why should I trust you? explaining the predictions of any classifier, in: *Proceedings of the 22nd ACM SIGKDD international conference on knowledge discovery and data mining*, 2016, pp. 1135–1144.
- [19] M. T. Ribeiro, S. Singh, C. Guestrin, Anchors: High-precision model-agnostic explanations, in: *Proceedings of the AAAI conference on artificial intelligence*, Vol. 32, 2018.
- [20] S. Wachter, B. Mittelstadt, C. Russell, Counterfactual explanations without opening the black box: Automated decisions and the gdpr, *Harv. JL & Tech.* 31 (2017) 841.
- [21] M. Sundararajan, A. Taly, Q. Yan, Axiomatic attribution for deep networks, in: *International conference on machine learning*, PMLR, 2017, pp. 3319–3328.
- [22] A. Ignatiev, Y. Izza, P. J. Stuckey, J. Marques-Silva, Using maxsat for efficient explanations of tree ensembles, in: *Proceedings of the AAAI Conference on Artificial Intelligence*, Vol. 36, 2022, pp. 3776–3785.
- [23] H. Sun, Y. Liu, A. Al-Tahmeesschi, A. Nag, M. Soleimanpour, B. Canberk, H. Arslan, H. Ahmadi, Advancing 6g: Survey for explainable ai on communications and network slicing, *IEEE*

Open Journal of the Communications Society 6 (2025) 1372–1412.
doi:10.1109/OJCOMS.2025.3534626.

- [24] H. Ouifak, A. Idri, A comprehensive review of fuzzy logic based interpretability and explainability of machine learning techniques across domains, *Neurocomputing* (2025) 130602.
- [25] G. Schwalbe, B. Finzel, A comprehensive taxonomy for explainable artificial intelligence: a systematic survey of surveys on methods and concepts, *Data Mining and Knowledge Discovery* 38 (5) (2024) 3043–3101.
- [26] M. Mersha, K. Lam, J. Wood, A. K. Alshami, J. Kalita, Explainable artificial intelligence: A survey of needs, techniques, applications, and future direction, *Neurocomputing* 599 (2024) 128111.
- [27] S. M. Lundberg, S.-I. Lee, A unified approach to interpreting model predictions, in: *Proceedings of the 31st International Conference on Neural Information Processing Systems (NeurIPS)*, 2017, p. 4768–4777.
- [28] J. Marques-Silva, Logic-based explainability: past, present and future, in: *International Symposium on Leveraging Applications of Formal Methods*, Springer, 2024, pp. 181–204.
- [29] X. Huang, J. Marques-Silva, On the failings of shapley values for explainability, *International Journal of Approximate Reasoning* (2024) 109112.
- [30] J. Marques-Silva, X. Huang, Explainability is not a game, *Commun. ACM* 67 (7) (2024) 66–75. doi:10.1145/3635301.
URL <https://doi.org/10.1145/3635301>
- [31] J. Törnblom, E. Karlsson, S. Nadjm-Tehrani, Finding minimum-cost explanations for predictions made by tree ensembles, *In Print* (2025).
URL [diva2:1953715](https://doi.org/10.1145/3635301)
- [32] S. Bassan, G. Katz, Towards formal XAI: formally approximate minimal explanations of neural networks, in: *International Conference on Tools and Algorithms for the Construction and Analysis of Systems*, Springer, 2023, pp. 187–207.
- [33] J. Marques-Silva, Logic-based explainability in machine learning, in: *Reasoning Web. Causality, Explanations and Declarative Knowledge:*

18th International Summer School 2022, Berlin, Germany, September 27–30, 2022, Tutorial Lectures, Springer, 2023, pp. 24–104.

- [34] K. Främling, Decision theory meets explainable ai, in: International workshop on explainable, transparent autonomous agents and multi-agent systems, Springer, 2020, pp. 57–74.
- [35] A. B. Arrieta, N. Díaz-Rodríguez, J. Del Ser, A. Bennetot, S. Tabik, A. Barbado, S. García, S. Gil-López, D. Molina, R. Benjamins, et al., Explainable artificial intelligence (XAI): Concepts, taxonomies, opportunities and challenges toward responsible AI, *Information fusion* 58 (2020) 82–115.
- [36] S. Samarakoon, Y. Siriwardhana, P. Porambage, M. Liyanage, S.-Y. Chang, J. Kim, J. Kim, M. Ylianttila, 5G-NIDD: A comprehensive network intrusion detection dataset generated over 5G wireless network (2022). doi:10.21227/xtep-hv36.
URL <https://dx.doi.org/10.21227/xtep-hv36>
- [37] K. S. Mubasshir, I. Karim, E. Bertino, Gotta detect 'em all: Fake base station and multi-step attack detection in cellular networks, in: Proceedings of the 34th USENIX Security Symposium, 2025.
- [38] G. Amponis, P. Radoglou-Grammatikis, T. Lagkas, W. Mallouli, A. Cavalli, D. Klonidis, E. Markakis, P. Sarigiannidis, Threatening the 5g core via PFCP DoS attacks: the case of blocking UAV communications, *EURASIP Journal on Wireless Communications and Networking* 2022 (1) (2022) 124.
- [39] E. C. P. Neto, S. Dadkhah, R. Ferreira, A. Zohourian, R. Lu, A. A. Ghorbani, Ciciot2023: A real-time dataset and benchmark for large-scale attacks in iot environment, *Sensors* 23 (13) (2023) 5941.
- [40] H. Mohammadian, A. H. Lashkari, A. A. Ghorbani, Poisoning and evasion: Deep learning-based nids under adversarial attacks, in: 2024 21st Annual International Conference on Privacy, Security and Trust (PST), IEEE, 2024, pp. 1–9.
- [41] E. Edozie, A. N. Shuaibu, B. O. Sadiq, U. K. John, Artificial intelligence advances in anomaly detection for telecom networks, *Artificial Intelligence Review* 58 (4) (2025) 100.

- [42] M. Pawlicki, A. Pawlicka, F. Uccello, S. Szelest, S. D'Antonio, R. Kozik, M. Choraś, Evaluating the necessity of the multiple metrics for assessing explainable AI: A critical examination, *Neurocomputing* 602 (2024) 128282.
- [43] A. Warnecke, D. Arp, C. Wressnegger, K. Rieck, Evaluating explanation methods for deep learning in security, in: *2020 IEEE european symposium on security and privacy (EuroS&P)*, IEEE, 2020, pp. 158–174.
- [44] D. Alvarez Melis, T. Jaakkola, Towards robust interpretability with self-explaining neural networks, *Advances in neural information processing systems* 31 (2018).
- [45] A. B. de Neira, B. Kantarci, M. Nogueira, Distributed denial of service attack prediction: Challenges, open issues and opportunities, *Computer Networks* 222 (2023) 109553.
- [46] A. Hirsi, M. A. Alhartomi, L. Audah, A. Salh, N. bin Mad Sahar, S. Ahmed, G. O. Ansa, A. Farah, Comprehensive analysis of ddos anomaly detection in software-defined networks, *IEEE Access* (2025).
- [47] D. Gaspar, P. Silva, C. Silva, Explainable AI for intrusion detection systems: Lime and shap applicability on multi-layer perceptron, *IEEE Access* 12 (2024) 30164–30175. doi:10.1109/ACCESS.2024.3368377.
- [48] S. Gyawali, J. Huang, Y. Jiang, Leveraging explainable AI for actionable insights in IoT intrusion detection, in: *2024 19th Annual System of Systems Engineering Conference (SoSE)*, 2024, pp. 92–97. doi:10.1109/SOSE62659.2024.10620966.
- [49] C. S. Kalutharage, X. Liu, C. Chrysoulas, Neurosymbolic learning and domain knowledge-driven explainable ai for enhanced iot network attack detection and response, *Computers & Security* 151 (2025) 104318.
- [50] D. Choi, J. Rheey, H. Park, Attack-specific feature analysis framework for netflow iot datasets, *Computers & Security* (2025) 104536.
- [51] M. Najibi, A. J. Bidgoly, Towards a robust android malware detection model using explainable deep learning, *Journal of Information Security and Applications* 93 (2025) 104191.

- [52] H. V. Vo, H. P. Du, H. N. Nguyen, Mdob: Enhancing resilient and explainable ai-powered malware detection using feature set optimization and mutual deep+ boosting ensemble inference, *Journal of Information Security and Applications* 93 (2025) 104175.
- [53] A. Drichel, U. Meyer, False sense of security: leveraging xai to analyze the reasoning and true performance of context-less dga classifiers, in: *Proceedings of the 26th international symposium on research in attacks, intrusions and defenses*, 2023, pp. 330–345.
- [54] O. T. Basaran, F. Dressler, XAIomaly: Explainable, interpretable and trustworthy AI for xurllc in 6G open-ran, in: *2024 3rd International Conference on 6G Networking (6GNet)*, IEEE, 2024, pp. 93–101.
- [55] A. Terra, R. Inam, S. Baskaran, P. Batista, I. Burdick, E. Fersman, Explainability methods for identifying root-cause of SLA violation prediction in 5G network, in: *GLOBECOM 2020-2020 IEEE Global Communications Conference*, IEEE, 2020, pp. 1–7.
- [56] C. Fiandrino, L. Bonati, S. D’Oro, M. Polese, T. Melodia, J. Widmer, EXPLORA: AI/ML explainability for the open RAN, *Proceedings of the ACM on Networking 1 (CoNEXT3)* (2023) 1–26.
- [57] V. O. Colaco, S. Nadjm-Tehrani, Fast evasion detection & alert management in tree-ensemble-based intrusion detection systems, in: *2024 IEEE 36th International Conference on Tools with Artificial Intelligence (IC-TAI)*, IEEE, 2024, pp. 404–412.

Appendix A List of Features

Table 3 and 4 present a subset of the most relevant network flow features identified across the explainability methods applied in this study, for 5G-NIDD and MSA, respectively.

Appendix B XGBoost Classifier Hyperparameters

Table 5 shows the final set of hyperparameters for the ML Classifiers employed in this study.

Appendix C False Positive Analysis

To complement the main TP-focused evaluation, we performed a detailed review of all FPs cases in the 5G-NIDD dataset. As shown in Table 2, the model produced only 37 FPs (benign flows misclassified as malicious).

For benign flows that were flagged, both methods surface traffic-shape and basic header cues. SHAP emphasizes byte/size and TTL indicators together with simple protocol markers (`TotBytes`, `sTtl`, `sMeanPktSz`, `INT`, `Offset`). VoTE-XAI frequently includes `Seq`, but does not bring in path/handshake structure (e.g., `dTtl`, `SynAck`, `dHops`). This suggests that the FPs could be benign bursts that mimic DoS-like shape, without the footprint seen in actual attacks. In light of the experiments, a consistent pattern emerges: (i) for TPs, traffic-shape features co-occur with sequence/fragmentation and path/handshake cues in both explainability methods (for the UDPFlood class); (ii) FPs lack this structural footprint.

In a live mitigation session, there is a further need to work out which subset of the positive class constitutes likely false positives. This is a fundamental problem since such cases by definition reside on the border of attacks and benign data. Initial approaches in the attack evasion context have been explored [57], whereby a subset of flows (likely FPs) can be prioritized lower by the operator, given some pre-analysis before run-time deployment.

Appendix D Summary of Stability

Table 6 and 7 detail feature importance across the three use cases for SHAP and VoTE-XAI, respectively.

Appendix E Summary of Divergence

Table 8 details the divergence between SHAP attribution and VoTE-XAI occurrences.

Table 3: Description of the most meaningful features according to both methods for the 5G-NIDD dataset.

Feature	Description
cs0	Quality of Service metric in the IP header (default best-effort service class).
dHops	Number of hops from destination (255 - dTtl).
DstBytes	Total bytes sent from the destination to the source.
DstTCPBase	Destination TCP base sequence number (initial sequence number used by the destination in the TCP connection).
DstWin	Destination TCP window advertisement value.
dTtl	Destination to source Time-to-Live value.
Dur	Total duration of the flow in seconds.
ECO	ICMP Echo Request (Ping request).
FIN	TCP connection termination flag.
INT	Initial transaction state (seen in UDP flows when the first packet is detected).
Load	Total bits per second for the flow (Sload + Dload).
Loss	Total packets lost (sloss + dloss).
Offset	Fragmentation offset value in the IP header.
pLoss	Number of packets lost from source to destination.
Rate	Total bits per second (same as Load).
REQ	TCP connection request (SYN seen, connection attempted).
RST	TCP connection reset (rejected or forcibly closed).
Seq	Flow sequence number.
sHops	Number of hops from the source (255 - sTtl).
sMeanPktSz	Mean size of packets transmitted by the source.
SrcBytes	Total bytes sent from the source to the destination.
SrcLoad	Source bits per second (Sload).
SrcPkts	Number of packets sent from the source to the destination.
SrcRate	Source bits per second (Sload).
SrcTCPBase	Source TCP base sequence number (initial sequence number used by the source).
SrcWin	Source TCP window advertisement value.
Start	Timestamp when the flow started.
sTtl	Source to destination Time-to-Live value.
SynAck	Time between SYN and SYN-ACK during TCP handshake.
TotBytes	Total bytes transferred (SrcBytes + DstBytes).
TotPkts	Total packets transferred (SrcPkts + Dpkts).
udp	Flow uses UDP protocol.

Table 4: Description of the most meaningful feature groups according to both methods for the MSA dataset.

Feature Group	Description
NAS EPS EMM	Handles LTE mobility management: attachment, tracking area update, UE identification, and EMM state transitions. Useful for detecting rogue base stations and tracking anomalies. Includes: F6: nas-eps-emm-id-type2-unmaskedvalue, F13: nas-eps-emm-guti-type-size, F16: nas-eps-emm-128eea1-unmaskedvalue, F20: nas-eps-emm-switch-off-size, F21: nas-eps-emm-id-type2-size.
NAS Security	Monitors NAS-level ciphering and integrity algorithms. Essential for identifying weak security configurations. Includes: F8: nas-eps-security-header-type-value, F17: nas-eps-msg-auth-code-show.
NAS Identifiers E.212	Contains global subscriber/operator identifiers. Useful for profiling and roaming analysis. Includes: F4: e212_gummei_mcc_size, F10: e212-tai-mnc-value, F23: e212-tai-mnc-show, F25: e212-tai-mnc-unmaskedvalue.
NAS Message Internals Encoding	Represents NAS message structure and encoding behavior. Helps detect malformed messages or optional feature usage. Includes: F7: nested-field2-value, F12: nested-field1-value, F14: nested-field1-show.
GSM A / DTAP (2G/3G Signaling)	Legacy 2G/3G signaling for mobility and authentication. Important for inter-RAT handover and fallback analysis. Includes: F1: gsm-a-oddevenind-unmaskedvalue, F2: gsm-a-spare-bits-unmaskedvalue, F22: gsm-a-dtap-add-ci-value, F24: gsm-a-extension-size.
ASN.1 Encoding Diagnostics	Captures encoding metadata and diagnostic flags. Important for debugging and feature engineering.

Table 5: Hyperparameters of the XGBoost Classifiers, selected using the best ones from RandomizedSearchCV.

Hyperparameter	Value	Description
scale_pos_weight	2.2	Balances the positive and negative classes to handle class imbalance.
n_estimators	100	The number of boosting rounds (trees) in the model.
max_depth	10	Maximum depth of a tree, controlling model complexity and risk of overfitting.
learning_rate	0.35	Step size shrinkage to prevent overfitting and adjust the weight of new trees.

Table 6: Globally and attack-specific important features according to SHAP.

Use Case	Feature	Details	Importance
Global Importance			
5G-NIDD	Seq (Sequence Number)	Highest across all attack types	Mean SHAP: 3.1–4.3
	Offset (Fragmentation Offset)	High in UDPFlood, SYNScan, ICMPFlood	Mean: 3.24, 3.60, 3.26
	sTtl (Source TTL)	Relevant in UDPFlood, HTTPFlood, SYNflood	Mean: 1.6–2.0
MSA	NAS Security features	Across most attack types	Mean: 0.17–1.83
	NAS Identifiers & E.212	Half of attack types	Mean: 0.10–0.31
	GSM A / DTAP	Several DoS attacks	Mean: 0.63–1.31
PFCP	Fwd IAT Min	All attack types	Mean: 0.71–0.98
	Dst IP	Frequent in top 5	Mean: 0.55–0.69
	Src IP	Several classes	Mean: 0.51–0.83
	Fwd Pkts/s	Most classes	Mean: 0.40–0.45
Attack-Specific Importance			
5G-NIDD	sMeanPktSz	SYNFlood	Mean: 3.80; Min: 1.05; Max: 8.28
	TotBytes	ICMPFlood	Mean: 5.99 (constant)
MSA	NAS Security (F23)	NAS Counter Desynchronization	Mean: 0.20; Max: 0.27
	NAS Identifiers & E.212 (F25)	Incarceration with rrcReestablishReject	Mean: 0.09; Max: 0.24
PFCP	Pkt Len Std	Session Establishment Flood	Mean: 0.586 (constant)
	Dst Port	Session Modification Flood (DROP)	Mean: 0.26; Min: 0.00; Max: 0.46

Table 7: Globally and attack-specific important features according to VoTE-XAI

Use Case	Feature	Details	Importance / Occurrence
Global Importance			
5G-NIDD	Seq	All minimal explanations (except UDPScan)	100% (85% in UDPScan)
	sTtl	All attack types (except SYNflood)	100% (68% in SYNflood)
	Offset	Top feature across attack types	Near-perfect
MSA	NAS Security, NAS EPS EMM, NAS Message Internals Encoding	Nearly all attack classes	100%
	NAS Identifiers E.212	Authentication Relay, Bidding Down with AttachReject, Handover Hijacking	99–100%
PFCP	Fwd IAT Min	Almost every attack class	93–100%
	Flow IAT Max, Flow IAT Std	Multiple attack types	33–38%
	Bwd/Pkts per Second	All attacks	34–37%
Attack-Specific Importance			
5G-NIDD	ECO (Ping request)	SlowrateDoS, HTTPFlood; low in scans and ICMPFlood	92.3%, 96.4%; low: 4.6–10.4%
	SynAck (SYN-ACK Time in Handshake)	SYNScan, UDPFlood, ICMPFlood,	72.4%–93.7%
	sMeanPktSz (Mean Packet Size)	SYNScan, UDPScan, TCPConnectScan, UDPFlood	100%
	cs0 (Class of Service)	Scan attacks, SlowrateDoS	89% in UDPScan 91% in SlowrateDoS
MSA	F8	Only NAS Desynch	Near perfect frequency
	F21	Bidding Down via TAURreject and AttachReject	Consistently high
PFCP	–	No attack specific features identified	–

Table 8: Summary of divergence between VoTE-XAI and SHAP feature importance across use cases.

Use Case	Feature(s)	VoTE-XAI Observation	SHAP Observation
5G-NIDD	dTtL	Critical in multiple attacks (82.8–99% occurrence)	Mean importance = 0 for most; 0.64 in SlowrateDoS, 0.48 in SYNflood
	ECO	92.3% in SlowrateDoS; 96% in HTTPflood	Mean importance \approx 0.24
	TotBytes	\approx 92% in SYNScan minimal explanations	Mean importance \approx 0
	cs0	Appears in almost all minimal explanations	Near 0 importance across all attacks
	SynAck	85.7–93.7% in SYNflood, TCPConnectScan, UDPScan	Near 0 mean value
	General trend	All top-ranked SHAP features appear in VoTE-XAI explanations	VoTE-XAI-only features often missed
MSA	GSM A / DTAP, NAS Security, NAS Identifiers E.212	100% inclusion in Authentication Relay	Mean importance < 0.07
	NAS EPS EMM, NAS Message Internals Encoding	100% in Bidding Down with AttachReject	Mean importance \approx 0.14, 0.11
PFCP	Fwd IAT Min	92.7% occurrence in DUPL flood	Mean SHAP: 0.80 (agreement)
	Bwd Pkts/s	33.9% in DUPL; frequent across floods	Mean SHAP: 0.0023
	Flow IAT Max	33.7% in DUPL; 37.5% in Session Establishment Flood	Mean SHAP: 0.0009
	Flow IAT Std	>33% occurrence across floods	Near-zero attribution